

Transient carrier decay and transport properties in $\text{Hg}_{1-x}\text{Cd}_x\text{Te}$

G. Nimtz, G. Bauer,* R. Dornhaus, and K. H. Müller

II. Physikalisches Institut der Universität zu Köln, D-5 Köln, Germany

(Received 28 November 1973)

The transient decay of large excess-carrier densities was investigated in $\text{Hg}_{1-x}\text{Cd}_x\text{Te}$ ($x=0.205$) at 77 K. Excess carriers were generated by bulk impact ionization in strong electric fields. A strong variation of the carrier lifetime with excess-carrier density was observed in the transient excess-carrier decay. The comparison with calculated values shows that the carrier decay is determined by the Auger recombination process. To our knowledge this is the first observed Auger-dominated transient carrier decay in a semiconductor. A typical Auger-dominated lifetime for carriers at excess-carrier densities not far from thermal equilibrium is 460 nsec for $n_0=9\times 10^{14}\text{ cm}^{-3}$ and $\mu_H=2.26\times 10^5\text{ cm}^2/\text{V sec}$ at 77 K. This lifetime decreased to 90 nsec at an excess-carrier density equal to n_0 . Photoconductivity experiments indicate that the majority-carrier lifetime can be enlarged due to minority-carrier trapping near contacts. This was established in photoresponse measurements with CO_2 laser pulses. In addition to this, the Hall mobility was measured and analyzed between 4.2 and 200 K. Calculations for combined ionized-impurity and polar-optical-phonon scattering indicate that above 77 K the polar-optical-phonon scattering limits the mobility. This electron-phonon interaction was calculated taking into account the two-mode behavior of $\text{Hg}_{1-x}\text{Cd}_x\text{Te}$. The high-field measurements have shown that in electric fields above 150 V/cm impact ionization occurs. Values of the carrier generation rate of $\text{Hg}_{0.8}\text{Cd}_{0.2}\text{Te}$ were deduced from the time dependent $j(E)$ characteristics.

I. INTRODUCTION

The determination of the electronic properties of the II-VI compound $\text{Hg}_{1-x}\text{Cd}_x\text{Te}$ has been the aim of many investigations in recent years.^{1,2} The strong interest in this mixed crystal was mainly due to its excellent characteristics for infrared detectors.³ The lifetime of the photoionized excess carriers represents a very important factor, for it determines directly the detectivity and the rise-time of the detectors. Quite recently this physical property was studied theoretically by Petersen⁴ and experimentally by Kinch, Brau, and Simmons.⁵ In the experimental investigation⁵ the dependence of the lifetime on the temperature was measured in order to characterize the relevant recombination mechanisms. Usually those experiments are carried out at small deviations from the thermal-equilibrium carrier density, since only then the lifetime has a constant value.

A different way to identify the relevant recombination mechanisms is to study the influence of the excess-carrier density on the lifetime. Similarly to the temperature dependence of the quasi-equilibrium lifetime, the dependence of the lifetime on the excess-carrier density is a characteristic of the dominant recombination mechanism.⁶ A microwave technique was introduced by Nimtz^{7,8} to study the density dependence of the carrier lifetime. In this technique the excess carriers are generated by bulk impact ionization in high electric fields instead of by photoionization. The transient carrier decay is measured by using microwaves. This experimental method yields directly the car-

rier lifetime dependence on the excess carriers. In addition, the photoconductivity response to CO_2 laser pulses is measured. The photoconductivity lifetime deduced from these experiments is compared with the lifetime of the impact-ionized carriers using the microwave technique.

One expects that in high-quality $\text{Hg}_{0.8}\text{Cd}_{0.2}\text{Te}$ the recombination is dominated by the Auger mechanism, since the band gap is relatively small.^{4,5} To our knowledge no experimental data of a transient carrier decay dominated by the Auger process in semiconductors have been published. $\text{Hg}_{0.8}\text{Cd}_{0.2}\text{Te}$ seems to be a suitable material for an Auger-dominated density-dependent carrier decay using the just-mentioned experimental technique.

Impact ionization in electric fields of the order of 100–1000 V/cm has been observed in semiconductors with small band gaps as, e. g., indium-antimonide⁹ and tellurium.⁷ Besides a small band gap, impact ionization is favored by a carrier-scattering mechanism which allows a strong carrier heating in the electric field.¹⁰ Therefore we have first investigated the Ohmic carrier mobility in the temperature range between 4.2 and 200 K in high-mobility n -type $\text{Hg}_{0.8}\text{Cd}_{0.2}\text{Te}$ and analyzed the relevant carrier-scattering mechanisms. Near the temperature of liquid nitrogen, the dominant scattering process was found to be the polar-optical-phonon scattering. Unlike the well-known semiconductors with predominant polar-optical-phonon scattering, e. g., GaAs or InSb, in the two-mode mixed crystal $\text{Hg}_{1-x}\text{Cd}_x\text{Te}$ we have to take into account the electron-phonon interaction with two distinct phonons. This peculiarity of a two-mode

TABLE I. Sample identification ($T=77$ K, $x=0.205$).

Sample No.	Carrier concentration n_0 (10^{15} cm $^{-3}$)	Hall mobility (μ_H) (cm 2 V $^{-1}$ sec $^{-1}$)	Resistivity (Ω cm)	Impact	Lifetime τ_0 (10^{-6} sec)	
					Photo	
N1, N2	0.965	0.3×10^5	22.0×10^{-2}	0.50	0.45	
N4, N5	0.6	1.25×10^5	8.35×10^{-2}	1.2	1.3	
N11	0.9	2.26×10^5	2.96×10^{-2}		0.46	

crystal is discussed, and the effect on the carrier mobility calculated and compared with the experimental results. It is worthwhile to mention that $\text{Hg}_{1-x}\text{Cd}_x\text{Te}$ is a mixed crystal which represents an exception of the atomic-mass criterion given by Chang and Mitra¹¹ for single- and two-mode behavior.

Recently Ancker-Johnson and Dick¹² investigated hot-carrier effects in $\text{Hg}_{1-x}\text{Cd}_x\text{Te}$. They observed a strong conductivity change above 100 V/cm and attributed it to an intervalley-transfer process. The experimental results reported in the present paper show a decrease of the conductivity with increasing electric field up to 150 V/cm, followed by a steep time-dependent increase. The non-Ohmic behavior can be explained by the polar-optical-scattering mechanism. Furthermore we show that the observed time dependence in the $j(E)$ characteristics is caused by an impact-ionization process.

In Sec. II, the sample preparation and the experimental arrangement is described. In Sec. III, first, experimental data on Ohmic conductivity and the Hall coefficient are presented and compared with calculations based on ionized impurity and polar optical scattering. This is followed by high-field data and the determination of the generation rate. Finally we present excess-carrier-lifetime values which are deduced from transient excess-carrier-decay measurements. The results are compared with calculations based on Auger and radiative-recombination mechanisms. The discrepancy between the results of the photoconductivity experiments by Kinch, Brau, and Simmons,⁵ and our results of the transient carrier decay is discussed.

II. EXPERIMENTAL METHODS

The experiments were carried out with various samples of n -type $\text{Hg}_{1-x}\text{Cd}_x\text{Te}$ ($x=0.205$, Cominco). The characteristics of the samples are listed in Table I and have been measured at a temperature of 77 K. Ohmic contacts were produced by soldering platinum wires of 0.07-mm diameter with In or $\text{In}_{0.8}\text{Cd}_{0.2}$ to the samples. The Hall data were deduced from experiments carried out with an ac van der Pauw method, the frequency of the applied current was 70 Hz. The current-field character-

istics were measured with voltage pulses of a 50- Ω delay-line generator at a repetition rate of 20 Hz (10–100-nsec pulse length, risetime ≤ 1 nsec). From the time dependence of the current-field characteristics, the generation rate of the impact-ionized carriers was calculated.⁹

The lifetime of the excess carriers was determined from the time-resolved microwave resistivity of the samples by using the following method: The investigated samples were in the shape of posts (diam ≈ 0.2 mm, length 6 mm) and were mounted in an X-band waveguide. The axes of the samples were aligned parallel to the electric field of the H_{10} mode. A sketch of the experimental arrangement is shown in Fig. 1. This arrangement is called an "inductive post" and the equivalent circuit is described in detail in the *Waveguide Handbook*.¹³ It was shown that the series impedances of the inductive post are much smaller than the shunt impedance for sample diameters much smaller than the inner dimensions of the waveguide, and for values of the relative complex dielectric constant of the investigated samples smaller than 100.¹⁴ These conditions are established for sample diameters of the order of 0.1 mm and an electrical resistivity of the order of 0.1 Ω cm. In this case the series impedances of the inductive post can be neglected and the calculations have shown that the ratio of incident to transmitted microwave power is a linear function of the sample resistivity.¹⁴ Thus, by measuring the transmitted microwave power during the decay of the excess carriers, the time dependence of the resistivity can be de-

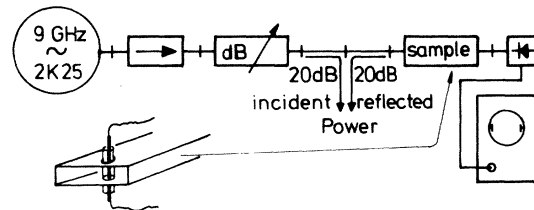


FIG. 1. Experimental arrangement for measuring the transient decay of impact-ionized excess carriers. The sample is located in a tapered X-band waveguide of 1-mm inner height.

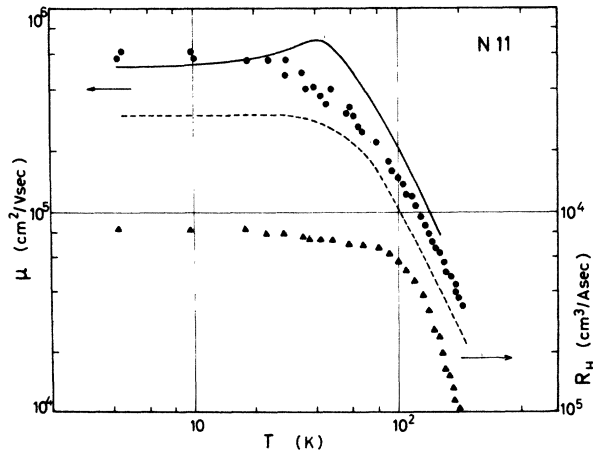


FIG. 2. Temperature dependence of the Hall mobility μ_H and of the Hall coefficient R_H (triangles) of sample N11. Solid curve: calculated values of conductivity mobility, dashed curve: experimental values on Hall mobility from Ref. 22.

duced. The time resolution of the microwave apparatus is less than 10 nsec. This microwave technique probes the sample on a length of 1 mm compared to a total sample length between 5 and 10 mm. (See Fig. 1).

The lifetime of excess carriers was also determined from transient photoconductivity experiments. Excess carriers were generated by 200-nsec CO_2 -laser pulses ($\lambda = 10.7 \mu\text{m}$, peak power 0.3 W). The excess-carrier density was less than 5% of the equilibrium carrier density. To eliminate any influence of the electrical contacts, e.g., as photovoltaic signals, the photoconductivity signal was measured at probes and not across the two current contacts. The probes and the current contacts were shaded from the laser radiation.

III. RESULTS AND ANALYSIS

A. Ohmic conductivity

In order to obtain information on the relevant scattering mechanisms, the Ohmic conductivity and the Hall effect were measured in the temperature range between 4.2 and 200 K. In Fig. 2 the experimental results are shown for the crystal with the highest mobility. Previous temperature-dependent investigations by several authors¹⁵⁻²¹ were carried out with crystals of lower mobility. It was shown by Long¹⁷ in an analysis of the mobility variation with composition x at 4.2 K, that ionized impurity scattering is dominant at helium temperatures. He has also discussed the limits of the Born approximation in calculating the mobility. An analysis of the temperature dependence of the mobility was performed later by Scott²² who con-

sidered ionized impurity scattering at low temperatures and electron-hole scattering at temperatures in excess of 100 K for a compound with $x = 0.2$. It has, however, been anticipated that polar-optical-phonon scattering will be of importance.

In analyzing the temperature dependence of the mobility in the small gap alloy $\text{Hg}_{1-x}\text{Cd}_x\text{Te}$ two important features have to be considered:

(a) In contrast to other zinc-blende materials the energy gap has a strong positive temperature coefficient^{1,23} for $x < 0.5$. From Kane's²⁴ theory this effect leads to a pronounced temperature dependence of the band-edge effective mass.

(b) $\text{Hg}_{1-x}\text{Cd}_x\text{Te}$ shows a two-mode behavior, e.g., optical phonons corresponding to HgTe- and CdTe-like phonons are observed at any given alloy composition.²⁵⁻²⁹ Therefore both longitudinal modes have to be included in the scattering probabilities. For the numerical calculation of $\mu_c(T)$ (the conductivity mobility) we have used the concept of a relaxation time although for polar scattering the conditions $T \ll \Theta$ or $T \gg \Theta$ (Θ being the Debye temperature¹⁰) are not fulfilled over the entire temperature range. A more elaborate variational solution should be deferred until the values of the coupling constants are known more precisely.

We use for ionized impurity scattering and for polar-optical-phonon scattering the expressions derived by Zawadzki and Szymanska^{30,31} for nonparabolic bands, modified to take into account a Fermi distribution at low lattice temperatures ($T \leq 60$ K). Values for the temperature dependence of the band-edge effective mass are taken from Ref. 32. The expressions for polar-mode scattering were modified to include two-mode behavior. The polar electron-phonon coupling is determined by the frequency-dependent dielectric constant of the system. This coupling can be characterized for each phonon mode by

$$E_0^i = m_c e 4\pi \rho^i(x) / \omega_{LO}^i, \quad (1)$$

where $i = 1, 2$ denotes the HgTe- and CdTe-like phonon mode ω_{LO} , respectively, m_c is the energy-dependent effective mass in the conduction band.³⁰ Values of the individual mode strengths $4\pi \rho^i(x)$ ³³ were deduced from infrared data given by Baars and Sorger.²⁵ It is experimentally proved that the mode strength decreases linearly with their fraction x in a compound as¹¹

$$\begin{aligned} 4\pi \rho^1(x) &= (1-x) 4\pi \rho_{\text{HgTe}}, \\ 4\pi \rho^2(x) &= x 4\pi \rho_{\text{CdTe}}. \end{aligned} \quad (2)$$

The values deduced by Eqs. (2) from data taken on pure HgTe and Cd are listed in Table II.

In order to obtain the total scattering rate we have added the scattering rates of both phonon modes with the same weight. This procedure is

TABLE II. Phonon mode parameter.

Mode	ω_{TO}^i (cm^{-1})	ω_{LO}^i (cm^{-1})	$4\pi\rho^i$ ($x=0$ or 1)	$4\pi\rho^i(x)$ ($x=0,2$)
1 (CdTe like)	149	156	3.2	0.64
2 (HgTe like)	121	137	5.8	4.64

reasonable with respect to the derivation of the above parameters and in respect of that the macroscopic random-element-isodisplacement model describes the two-mode behavior of the mixed crystals well.^{11,34} The mode strength represents a macroscopic value, in which the fraction of each compound is included.

The dependence of the conductivity mobility on T was calculated using the parameters of Tables I and II. The theoretical curve for ionized impurity scattering and polar scattering is shown in Fig. 2. For temperatures below 77 K the calculated data show a maximum which is not found experimentally in our high-mobility material (e.g., N11). The calculated maximum results from the decreasing scattering rate of ionized impurities with increasing T and the increasing rate of polar optical scattering with T . Such a behavior is observed both theoretically and experimentally in, e.g., InSb.³⁵ Previous investigations on HgCdTe samples exhibiting a somewhat lower mobility^{16,17,22} have found a maximum of the Hall mobility in the temperature range between 20 and 100 K. Looking for the cause of the missing extremum in our high-mobility material, we have estimated the influence of deformation potential and piezoelectric scattering but found that both mechanisms yield scattering rates too small to account for the disappearance of the extremum in our case. In our calculation of the ionized impurity scattering according to Ref. 3, which uses the Thomas-Fermi screening model including nonparabolicity, a temperature-independent static dielectric constant is used. There are some indications for a temperature dependence of the static dielectric constant. Transmission data of Carter *et al.*²⁷ yielded a value for $\epsilon_0 = 19.5$ at 4.2 K compared to 17.5 found by Baars and Sorger²⁵ at 77 K for a compound with $x = 0.2$. This temperature dependence of ϵ_0 would improve the agreement between the calculated and experimental values.

Above 100 K the material becomes intrinsic³⁶ as evidenced by the Hall-coefficient data, also shown in Fig. 2. The Hall measurements were carried out in a magnetic field of 500 G. Recently it has been suggested by Ohtsuki *et al.*³⁷ that there might be electronic conduction in the heavy-mass valence band of HgCdTe contributing to the conductivity. However, our field-dependent Hall data of sample

N11 shown in Fig. 3 (up to 10 kG) do not indicate such a behavior. In contrast to observations of Ohtsuki *et al.* only a small decrease of 30% up to 10 kG in the Hall coefficient was observed. But it should be pointed out that, similar to Ohtsuki *et al.*, our low-mobility samples show a strongly decreasing Hall coefficient with increasing magnetic field. Thus the change of the Hall coefficient with magnetic field might result from the same physical cause as the decreasing carrier mobility.

B. Impact ionization

Until now there have been only a few investigations in which the high-field behavior of HgCdTe was studied. In the early investigations,^{21,38} acoustic-phonon scattering was believed to dominate the field dependence of the mobility. Ancker-Johnson and Dick¹² also studied nonlinear conduction in HgCdTe but their results are, however, considerably influenced by inhomogeneity effects, as stated by the authors themselves. Up to now there was no clear evidence for an impact-ionization process in HgCdTe in high electric fields.^{12,39}

To fulfill the assumptions of the inductive post, as discussed in Sec. II the impact-ionization experiments were carried out only in high-resistivity samples. The dynamical behavior of the carrier heating in the electric field is shown in Fig. 4. A voltage pulse U_1 was applied to the sample while the microwave transmission of the sample was measured. The signal of the transmitted microwave power P_m is in first-order approximation proportional to the resistivity of the sample.^{7,8} Instantaneously with the applied voltage the sample resistivity increases due to the carrier heating.

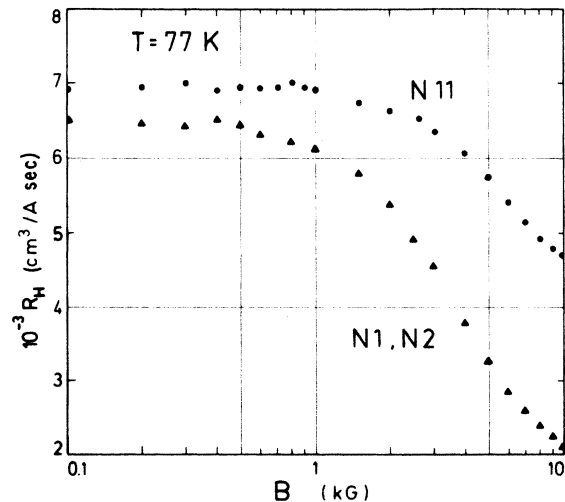


FIG. 3. Hall coefficient R_H as a function of magnetic field B for high-mobility sample N11 (dots) and low-mobility samples N1, N2 (triangles).

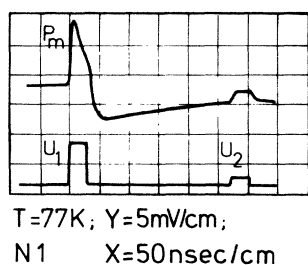


FIG. 4. Transmitted microwave power P_m vs time t . P_m is proportional to the sample resistivity. The lower trace represents the applied voltage pulses U_1 and U_2 both of 30-nsec length. The instantaneous increase of resistivity with U_1 and U_2 is due to the carrier heating in the electric field. The decrease, approximately 15 nsec after U_1 was applied, is due to impact ionization and corresponds to an excess-carrier generation of 30% of n_0 at the end of U_1 .

Since the small microwave electric field amplitude was parallel to the strong dc field pulse (U_1 corresponds to 300 V/cm), the increase of P_m represents the differential resistivity. About 15 nsec after the field was applied, the resistivity decreases due to impact ionization, causing an avalanche breakdown. After the end of the voltage pulse, the hot carriers thermalize within the energy relaxation time of the order of 10^{-12} sec and the remaining decrease is due to the excess carriers. Now we observe an increasing resistivity due to the excess-carrier decay. The microwave signal is modulated by a second but smaller voltage pulse U_2 . This

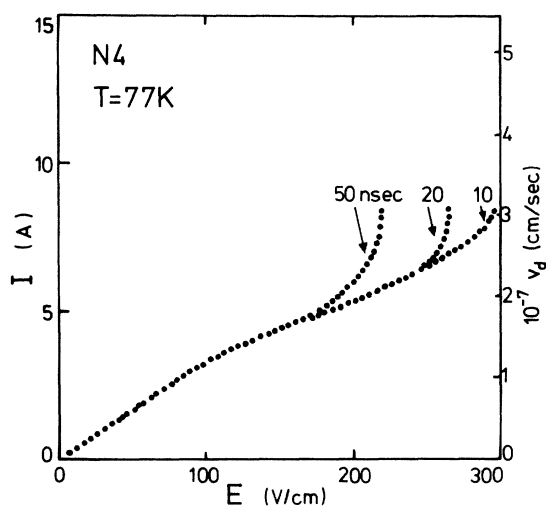


FIG. 5. $j(E)$ characteristic at 77 K of sample N4. Dotted line: experimental data. The data were recorded 10, 20, and 50 nsec after the electric field E was applied. The scale of the carrier drift velocity v_d is valid for the experimental data only up to $E \leq 160$ V/cm.

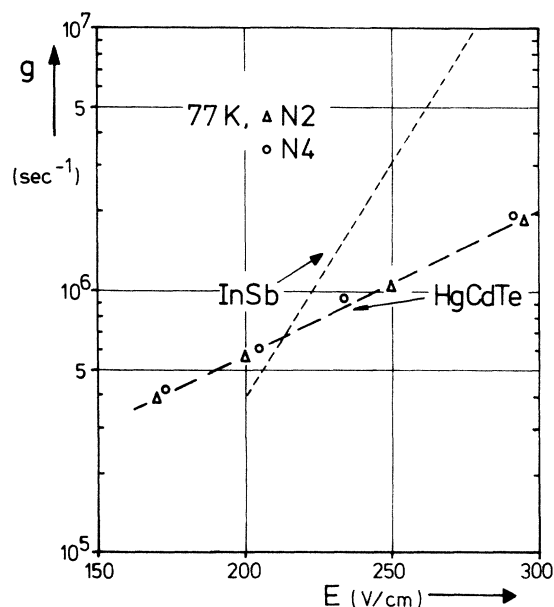


FIG. 6. Generation rate $g(E)$ as a function of electric field E . Experimental data of n -type $\text{Hg}_{0.8}\text{Cd}_{0.2}\text{Te}$ are compared with data of n -InSb (Ref. 9).

voltage is too small for impact ionization and the modulation is only due to the carrier heating and the connected increase of differential resistivity. This non-Ohmic behavior which was observed by the microwave transmission was also found in the dc characteristic $j(E)$, which is plotted in Fig. 5. Above fields of 90 V/cm deviations from Ohm's law occur and above 160 V/cm a time-dependent increase of the current density is observed. We bring the time-dependent avalanche breakdown at fields above 160 V/cm, which was observed in the microwave and in the dc resistivity, into relation with an excess-carrier generation due to impact ionization. This interpretation is supported by the fact that the relaxation of the breakdown in the electric field has the same time constant as the recombination time of photoionized carriers which is shown in the next section. From the time-dependent $j(E)$ characteristics we have calculated the generation rate of excess carriers by impact ionization as a function of the electric field according to⁹

$$g = \frac{1}{n} \frac{dn}{dt} = \frac{1}{j} \frac{dj}{dt}, \quad (3)$$

n and j are the instantaneous electron and current densities, respectively. Here it is assumed that the experiments were carried out with $E = (\text{const})$ and $v_d = (\text{const})$. The results are plotted in Fig. 6 as a function of the applied electric field E . The data can be fitted by a function of the form

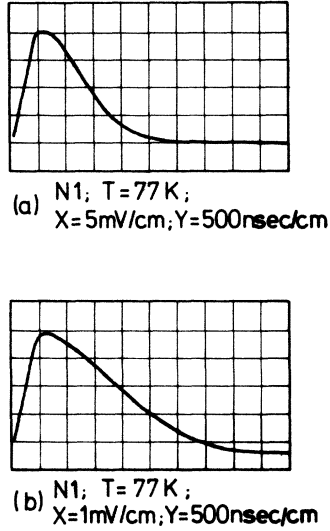


FIG. 8. Decay of photoconductive response to CO₂-laser pulses. The signals were measured with the laser radiation focused at the sample: (a) far from the electrical contacts and (b) in the contact region. The decay times are about (a) 500 nsec and (b) 1000 nsec.

carriers. Table I contains for comparison all the data observed by both experimental methods.

There are three recombination mechanisms in semiconductors which establish the thermodynamical equilibrium. These are the Shockley-Read mechanism, the radiative recombination of carriers, and the impact or so-called Auger recombination.⁶ To recognize the relevant recombination mechanism, usually in a steady-state experiment, the carrier lifetime and particularly the dependence of the lifetime on temperature is measured. The function $\tau_0(T)$ is characteristic of the effective recombination process. But similar to the temperature dependence, the lifetime shows a dependence on the number of nonequilibrium carriers which characterizes the recombination mechanism too.⁶

In a small-gap semiconductor like Hg_{0.8}Cd_{0.2}Te the Auger recombination might be important, since the recombination rate increases with decreasing band gap.⁴¹ Quite recently Petersen⁴ calculated the carrier lifetime for this recombination mechanism in Hg_{0.8}Cd_{0.2}Te and experimental results of the photoconductivity were interpreted by this mechanism.⁵ In our transient experiment we have measured directly the carrier lifetime and observed a strong decrease of the lifetime with increasing excess carrier density n_e as shown in Fig. 7. Assuming that Auger recombination is the most effective mechanism in the investigated material, we shall calculate the lifetime dependence on the excess-carrier density. For the transient decay of the carriers after the excitation process,

e. g., the impact ionization in the electric field, has ceased, we have the relation⁶

$$\frac{dn_e}{dt} = -\frac{n_e}{\tau} \quad (5)$$

$$= (g_{ee} - r_{ee}) + (g_{hh} - r_{hh}),$$

τ is the excess-carrier lifetime; r_{ee} , r_{hh} , g_{ee} , and g_{hh} are the rates of pair recombination and generation due to electron-electron and hole-hole collisions, respectively. With the assumptions that the carrier distribution is Maxwellian and the validity of microscopic reversibility, the non-equilibrium rates are related to the thermal equilibrium rates G_{ee} and G_{hh} as

$$r_{ee} = G_{ee} (n^2 p / n_0^2 p_0), \quad g_{ee} = G_{ee} (n / n_0), \quad (6)$$

$$r_{hh} = G_{hh} (n p^2 / n_0 p_0^2), \quad g_{hh} = G_{hh} (p / p_0).$$

These relations appear to be reasonable since in the recombination process there are three free carriers involved and in the generation only one. Thus we have for the carrier decay

$$\frac{dn_e}{dt} = -\frac{(np - n_i^2)(G_{ee} n p_0 + G_{hh} p n_0)}{n_i^4}. \quad (7)$$

Here n_i is the intrinsic carrier density, n_0 and p_0 are the thermal-equilibrium densities, and $n = n_0 + n_e$. Since $m_c \ll m_v$ in the investigated material, hh collisions can be neglected and Eq. (7) simplifies to

$$\frac{dn_e}{dt} = -\frac{n_e (n_0 + p_0 + n_e) G_{ee} n p_0}{n_i^4} \quad (8)$$

$$= -\frac{n_e (n_0 + p_0 + n_e)(n_0 + n_e)}{2 \tau_i n_i^2}.$$

τ_i represents the intrinsic Auger lifetime and is given by

$$\tau_i = n_i / (2 G_{ee}). \quad (9)$$

The generation rate of ee processes in thermal equilibrium is

$$G_{ee} = \left[\frac{8(2\pi)^{5/2} e^4 m_0}{h^3} \right] \left[\frac{(m_c/m_0) |F_1 F_2|^2}{\epsilon_s^2 (1 + m_c/m_v)^{1/2} (1 + 2 m_c/m_v)} \right]$$

$$\times n_0 \left(\frac{k_B T}{\mathcal{E}_g} \right)^{3/2} \exp \left[-\left(\frac{1 + 2 m_c/m_v}{1 + m_c/m_v} \right) \frac{\mathcal{E}_g}{k_B T} \right]. \quad (10)$$

This expression was found by Beattie and Landsberg⁴¹ and the symbols have the meaning: m_0 , m_c , and m_v are the free-electron, the conduction- and valence-band masses, respectively. \mathcal{E}_g is the gap energy, and F_1 and F_2 represent overlap integrals.⁴¹ Following the theory of Beattie and Landsberg, a value of $\tau_i = 8 \times 10^{-4}$ sec was calculated by Petersen⁴ for Hg_{0.8}Cd_{0.2}Te at 77 K. For $n_e \ll n_0$ the quasi-equilibrium lifetime $\tau = \tau_0$ is by Eqs. (5) and (8) in n -type material:

$$\tau_0 \approx 2\tau_i (n_i/n_0)^2. \quad (11)$$

From this relation a value of 1.4 μsec is expected in material with $n_0 = 10^{15} \text{ cm}^{-3}$ and $n_i = 3 \times 10^{13} \text{ cm}^{-3}$, where the intrinsic carrier density corresponds to $x = 0.2$.³⁶ The experimental results of τ_0 are in reasonable agreement with the theoretical values and they fulfill the dependence on n_0 of Eq. (11).

The transient-carrier decay as described by Eq. (8) is plotted in Fig. 7 and compared with the experimental results. Obviously the calculated steep increase of the recombination rate above 0.1 of n_e/n_0 was observed in the experiment. Blakemore⁶ calculated the transient-carrier decay of excess carriers due to radiative recombination. These values are also plotted for comparison in Fig. 7. Apart from the fact that a much larger lifetime is expected for this mechanism in $\text{Hg}_{0.8}\text{Cd}_{0.2}\text{Te}$ (approximately 20 μsec),⁵ the relative transient decay is much slower than that measured and that expected for the Auger decay.

Thus the transient decay has shown that Auger recombination is the dominant recombination mechanism in $\text{Hg}_{0.8}\text{Cd}_{0.2}\text{Te}$ at high excess-carrier densities. No other recombination mechanism is expected to have such a steep increase of the recombination rate with the excess-carrier density. Our observed lifetimes τ_0 are smaller up to a factor of 0.5 than those measured by Kinch *et al.*,⁵ if the dependence of τ_0 on n_0 is taken into account according to Eq. (11). We have observed similar long lifetimes, as shown in Fig. 8(b), when laser radiation was focused onto the sample near the contacts. Thus we conclude that the larger lifetimes may be caused by minority-carrier trapping in the contact region. These lifetimes were up to three times larger than those found by the microwave measurement in the bulk of the sample or with photoionization far from the contacts.

IV. CONCLUSION

The comparison of the experimental and theoretical data indicates that at low temperatures, ionized-impurity scattering, and at 77 K, polar-optical-phonon scattering governs the mobility. In

the polar-optical-phonon scattering the two-mode behavior of this mixed crystal was taken into account.

In high electric fields above 160 V/cm, a time-dependent increase of the current density occurs in a nsec time scale. This effect is explained by impact ionization, i. e., generation of electron-hole pairs in the electric field. This interpretation is confirmed by the fact that the avalanche breakdown of the current has the same decay time as photoionized carriers.

In order to study the lifetime the transient-carrier decay of impact-ionized carriers was investigated. By impact ionization, excess carriers are generated in the bulk of the sample in contrast to a photoionization technique, where the ionization process is more or less restricted to the surface.

The observed transient-carrier decay demonstrates a strong dependence on the excess-carrier density, as it is predicted from nonequilibrium statistical calculations for Auger recombination. To our knowledge this is the first observed density-dependent transient-carrier decay dominated by the Auger-recombination process. We have carried out for comparison also photoconductivity measurements with the same samples. These measurements have shown, that the excess-carrier decay is slowed down near the contacts. This effect might be interpreted by a trapping of minority carriers in the contact regions and may explain the moderate discrepancy by a factor of 2 between our results and those quoted in Ref. 5.

The nonstationary method of the transient decay of impact-ionized excess carriers has proved to be a valuable tool to supplement transport data in $\text{Hg}_{1-x}\text{Cd}_x\text{Te}$.

ACKNOWLEDGMENTS

We thank Prof. H. Happ, Dr. H. Kölker (Consortium, München), and Dipl. Phys. Stahl (AEG-Telefunken, Ulm) for valuable discussions. Dipl. Phys. Stahl supplied us with the $\text{Hg}_{0.8}\text{Cd}_{0.2}\text{Te}$ crystals. The work was supported by the Deutsche Forschungsgemeinschaft.

*Permanent address: I. Physikalisches Institut der Rheinisch Westfälischen Technischen Hochschule Aachen, Aachen, Germany.

¹C. Veri , in *Advances in Solid State Physics*, edited by O. Madelung (Pergamon-Vieweg, Braunschweig, 1970), Vol. x, p. 1.

²D. Long and J. L. Schmit, in *Semiconductors and Semimetals*, edited by R. K. Willardson and A. C. Beer (Academic, New York, 1970), Vol. 5, p. 175.

³I. Melngailis, in *Proceedings of the International Conference on the Physics of Semiconductors and Semimetals*, Nice, 1973 (unpublished).

⁴P. E. Petersen, *J. Appl. Phys.* **41**, 3465 (1970).

⁵M. A. Kinch, M. J. Brau, and A. Simmons, *J. Appl. Phys.* **44**, 1649 (1973).

⁶J. S. Blakemore, *Semiconductor Statistics* (Pergamon, New York, 1962).

⁷G. Nimtz, in *Proceedings of the International Conference on the Physics of Semiconductors*, Cambridge, 1970, edited by S. P. Keller, J. C. Hensel, and F. Stern (U.S. AEC, Oak Ridge, Tenn., 1970), p. 369.

⁸A. Bringer and G. Nimtz, *Phys. Status Solidi B* **46**, 235 (1971).

⁹J. C. McGroddy and M. I. Nathan, *J. Phys. Soc. Jap.*

- Suppl. 22, 437 (1967).
- ¹⁰E. M. Conwell, in *Solid State Physics*, edited by F. Seitz, D. Turnbull, and H. Ehrenreich (Academic, New York, 1967) Suppl. 9.
- ¹¹I. F. Chang and S. S. Mitra, *Adv Phys.* 20, 359 (1971); *Phys. Rev.* 172, 924 (1968).
- ¹²B. Ancker-Johnson and C. L. Dick, Jr., in *The Physics of Semimetals and Narrow Gap Semiconductors*, edited by D. L. Carter and R. T. Bate (Pergamon, New York, 1971), p. 461.
- ¹³N. Marcuvitz, *Waveguide Handbook*, Rad. Lab. Ser. No. 10 (Dover, New York, 1948), p. 266.
- ¹⁴K. Hess, G. Nimtz, and K. Seeger, *Solid State Electr.* 12, 79 (1969).
- ¹⁵M. Rodot, H. Rodot, and C. Veri , in *Proceedings of the International Conference on the Physics of Semiconductors, Paris 1964*, edited by M. Hulin (Dunod, Paris, 1964), p. 1237.
- ¹⁶C. T. Elliott and I. L. Spain, *Solid State Commun.* 8, 2063 (1970).
- ¹⁷D. Long, *Phys. Rev.* 176, 923 (1968).
- ¹⁸B. L. Gel'mont, V. I. Ivanov-Omskii, B. T. Kolomiets, V. K. Ogorodnikov, and K. P. Smekalova, *Fiz. Tekh. Poluprovodnikov* 5, 266 (1971) [*Sov. Phys.-Semicond.* 5, 228 (1971)].
- ¹⁹J. Stankiewicz, W. Giriat, and A. Bienenstock, *Phys. Rev. B* 4, 4465 (1971).
- ²⁰J. Stankiewicz and W. Giriat, *Phys. Status Solidi B* 48, 467 (1971).
- ²¹C. Veri , *Phys. Status Solidi* 17, 889 (1966).
- ²²W. Scott, *J. Appl. Phys.* 43, 1055 (1972).
- ²³P. W. Kruse, D. Long, and O. N. Tufte, in *Proceedings of the Third International Conference on Photoconductivity, Stanford, Calif.* 1969, edited by E. M. Pell (Pergamon, New York, 1971), p. 223.
- ²⁴E. O. Kane, *J. Phys. Chem. Solids* 1, 249 (1957).
- ²⁵J. Baars and F. Sorger, *Solid State Commun.* 10, 875 (1972).
- ²⁶R. S. Kim and S. Narita, *J. Phys. Soc. Jap.* 31, 613 (1971).
- ²⁷D. L. Carter, M. A. Kinch, and D. D. Buss, in Ref. 12, p. 273.
- ²⁸A. Mooradian and T. C. Harman, in Ref. 12, p. 297.
- ²⁹M. A. Kinch and D. D. Buss, in Ref. 12, p. 461; B. D. McCombe and R. J. Wagner, in *Proceedings of the International Conference on the Physics of Semiconductors, Warsaw, 1972* (PWN-Polish Scientific Publishers, Warsaw, 1972), p. 321.
- ³⁰W. Zawadzki and W. Szymanska, *Phys. Status Solidi B* 45, 415 (1971).
- ³¹H. Kahlert and G. Bauer, *Phys. Rev. B* 7, 2670 (1973).
- ³²H. Kahlert and G. Bauer, *Phys. Rev. Lett.* 30, 1211 (1973).
- ³³A. S. Barker, *Phys. Rev.* 145, 391 (1966).
- ³⁴Y. S. Chen, W. Shockley, and G. L. Pearson, *Phys. Rev.* 151, 648 (1966).
- ³⁵D. L. Rode, *Phys. Rev. B* 2, 1012 (1970).
- ³⁶J. L. Schmit, *J. Appl. Phys.* 41, 2876 (1970).
- ³⁷O. Ohtsuki, R. Ueda, and S. Narita, in Ref. 3.
- ³⁸M. Rodot, in *Proceedings of the International Conference on the Physics of Semiconductors, Moscow, 1968* (Publishing House Nauka, Leningrad, 1968), p. 639.
- ³⁹V. N. Kobzyev and A. S. Tager, *Zh. Teor. Fiz. Pis'ma Red.* 14, 164 (1971) [*JETP Lett.* 14, 107 (1971)].
- ⁴⁰W. P. Dumke, *Phys. Rev.* 167, 783 (1968).
- ⁴¹A. R. Beattie and P. T. Landsberg, *Proc. Roy. Soc. A* 249, 16 (1959).